Cs Fountain Clocks for Commercial Realizations—An Improved and Robust Design

Richard J. Hendricks, *Member, IEEE*, Filip Ozimek, Krzysztof Szymaniec, Bartłomiej Nagórny, Piotr Dunst, Jerzy Nawrocki, Scott Beattie, Bin Jian, and Kurt Gibble

***Abstract*— We report on the design, assembly, testing, and delivery of a series of new cesium fountain primary frequency standards built through commercial and scientific collaboration with international users. The new design, based on proven National Physical Laboratory solutions, improves reliability, simplicity of operation, and transportability. The complete system consists of a novel physics package, a specially developed optical package, and dedicated electronics for system control. We present results showing that despite their simplified and more compact design, the new fountains have state-of-the-art performance in terms of signal-to-noise ratio and robust long-term operation. With a sufficiently low-noise local oscillator, they are capable of reaching a short-term stability below 3×10^{-14} (1 s) and have potential accuracy in the low 10^{-16} range, similar to the best cesium fountains currently in operation. This cost-effective solution could be used to increase the availability of accurate frequency references and timescales and provide redundancy in critical locations.**

***Index Terms*— Atomic clocks, primary frequency standards, timescales.**

I. Introduction

ROBUST and accurate timescales are vital for a growing number of navigation, transport, financial, commercial, security, and scientific applications. The level of time stability and accuracy demanded by these sectors is growing, and as societies become more dependent upon them, the consequences of a loss of access to a high-quality timescale are becoming increasingly serious. Timescales accurate to nanoseconds are maintained in a few national laboratories and timing institutes, with satellite links and global navigation satellite systems used as the primary means of distributing precise time between laboratories and to end users. Since satellite links are vulnerable to failure, either through technical issues or intentional denial, resilience is becoming an increasing concern [1]. Optical fiber networks are being developed for very high stability timing applications [2], [3], and radio, 5G communication, and wireless networks have the potential to provide an alternative for accurate positioning [4], [5], but the relatively small number of primary timing laboratories makes long-range synchronization across such networks both challenging and vulnerable.

Currently, the most stable and accurate timescales use a combination of hydrogen maser clocks and atomic fountain frequency standards [6]–[8]. The masers provide excellent reliability and good short-term stability but exhibit long-term frequency drifts that limit their accuracy. Cesium atomic fountains are used as the primary frequency standards that correct for the maser frequency drift, providing long-term stability and accuracy by a direct realization of the SI second. Unlike masers, which have been commercially available for many years, atomic fountains have tended to require lengthy in-house development in time and frequency laboratories and needed frequent maintenance by experienced users. These development and maintenance costs have seriously limited the uptake of atomic fountain technology.

We have designed, built, and delivered several new cesium fountain systems to international users under commercial contract, while full analysis and accuracy evaluation will be performed with end users as part of a scientific collaboration. The design is based on an improved version of the two fountains currently operating at the National Physical Laboratory (NPL) in Teddington, U.K. It consists of a state-of-the-art physics package, shown in Fig. 1, a specially developed laser and optical package, shown in Fig. 2, and custom electronics for fountain control. The system has been designed to improve reliability, simplicity, and transportability without sacrificing stability and accuracy performance. As the first commercially available complete primary frequency standard, it is intended to be a cost-effective and low-maintenance system that could be used to extend the availability of accurate timescales to new geographical regions and improve redundancy in critical applications.

Up until now, two complete fountain systems of the new design, AOS-CsF1 and AOS-CsF2, have been delivered to the Astrogeodynamical Observatory (AOS) in Borowiec, Poland, and the Poznań Supercomputing and Networking

Manuscript received July 30, 2018; accepted October 2, 2018. Date of publication October 8, 2018; date of current version March 14, 2019. This work was supported in part by the U.K. Department of Business, Energy and Industrial Strategy through the National Measurement System Program, in part by the Polish Ministry of Science and Higher Education (Polish Atomic Clock—Cesium Fountain) under Grant IA/SP/0441/2015, and in part by the National Science Foundation. *(Corresponding author: Richard J. Hendricks.)*

R. J. Hendricks and K. Szymaniec are with the National Physical Laboratory, Teddington TW11 0LW, U.K. (email: rich.hendricks@npl.co.uk; krzysztof.szymaniec@npl.co.uk).

F. Ozimek was with the National Physical Laboratory, Teddington TW11 0LW, U.K. He is now with the UCL Mullard Space Science Laboratory, Dorking RH5 6NT, U.K.

B. Nagórny, P. Dunst, and J. Nawrocki are with the Space Research Centre, Astrogeodynamical Observatory, 62-023 Borowiec, Poland.

S. Beattie and B. Jian are with the National Research Council, Ottawa, ON K1A 0R6, Canada.

K. Gibble is with the Pennsylvania State University, State College, PA 16802 USA.

Digital Object Identifier 10.1109/TUFFC.2018.2874550

Fig. 1. Photograph of the AOS-CsF1 physics package—the first of the new NPL design to be assembled.

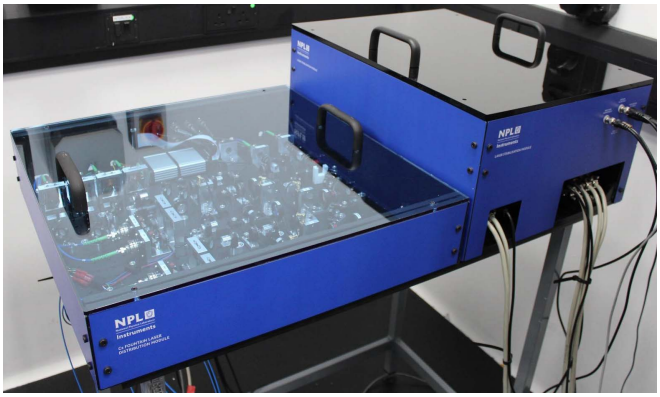

Fig. 2. Photograph of the first complete new NPL optical system, operated with AOS-CsF1.

Center (PSNC) in Poznań, Poland. A third physics package has been sent to the National Research Council (NRC) in Ottawa, ON, Canada, where it now forms an integral part of NRC-FCs2. The measurements presented throughout this paper are new data taken from these commercial systems and from the NPL fountain NPL-CsF3, which has been partially upgraded in line with the new design.

In this paper, we give a brief overview of the operating principle of these fountains, followed by a detailed description of some of the novel aspects of the physics package, optics, and electronics. Finally, we provide measurements of various aspects of system performance, with a view to estimating their potential stability, robustness, and accuracy.

II. Fountain Operation

The general principles behind the operation of Cs fountains have been described earlier [9], [10]. Although they all feature the capturing, laser cooling, and vertical launch of a cloud of atoms, followed by two passes through a microwave interaction region and subsequent measurement of the atomic states, the specific designs of fountains that have been built in different laboratories vary greatly. For example, the various systems produce the sample of cold cesium atoms and prepare them in the required atomic state in different ways. A range of approaches also minimize or control systematic effects such as cold collisions [11], [12], blackbody radiation [13], microwave leakage [14], [15], and distributed phase effects [16], [17] in the microwave resonator.

The methods used to address these problems in the NPL fountains are technically relatively simple and, hence, are well suited for use in a fountain designed to be reliable, robust, and simple to maintain and operate. Detailed descriptions of these fountains have appeared elsewhere [18], [19], and only the key attributes of the fountain cycle are described briefly here. Most of the internal components of the new physics package design described are visible in the rendering in Fig. 3.

The fountains directly load cesium atoms into a magneto-optical trap (MOT) from a vapor produced by a cooled reservoir of cesium metal. This simple, single-stage, 0-0-1 configuration MOT consists of three pairs of counter-propagating laser beams, two horizontal and one vertical, centered on the zero of a quadrupolar magnetic field. One of the beams also contains repumper light. After an atom accumulation phase, the quadrupolar magnetic field is pulsed off and a brief molasses phase cools the atoms to about 1 μK. The initial atom cloud size is tuned with a short dark period of variable duration before the molasses cooling. The atom cloud is launched vertically with a precisely defined velocity by a moving molasses technique. The atoms are then illuminated with a π-polarized light pulse tuned near the $S_{1/2}\,|F=4\rangle \longrightarrow P_{3/2}\,|F=4\rangle$ transition and optically pumped into $|F=4, m_F=0\rangle$, one of the magnetically insensitive "clock" states [20]. This optical pumping pulse leads to a fivefold increase in the detected clock state population. Finally, the cloud continues its ballistic trajectory into the microwave spectroscopy region in the flight tube.

The flight tube consists of two microwave resonators and a free-flight zone, all within a highly uniform magnetic field (the C-field) formed by a solenoid. The C-field lifts the degeneracy of the magnetic sublevels of the ground hyperfine states. The flight tube is temperature controlled to within about 100 mK by a water jacket and is surrounded by three layers of magnetic shielding. A pulse of microwaves in the lower "state selection" resonator transfers population from $|F=4, m_F=0\rangle$ to the $|F=3, m_F=0\rangle$ state. The 20%–30% of the atoms that remain in other sublevels of the $F=4$ state after optical pumping are expelled from the cloud by pushing them with a resonant light pulse. The state prepared

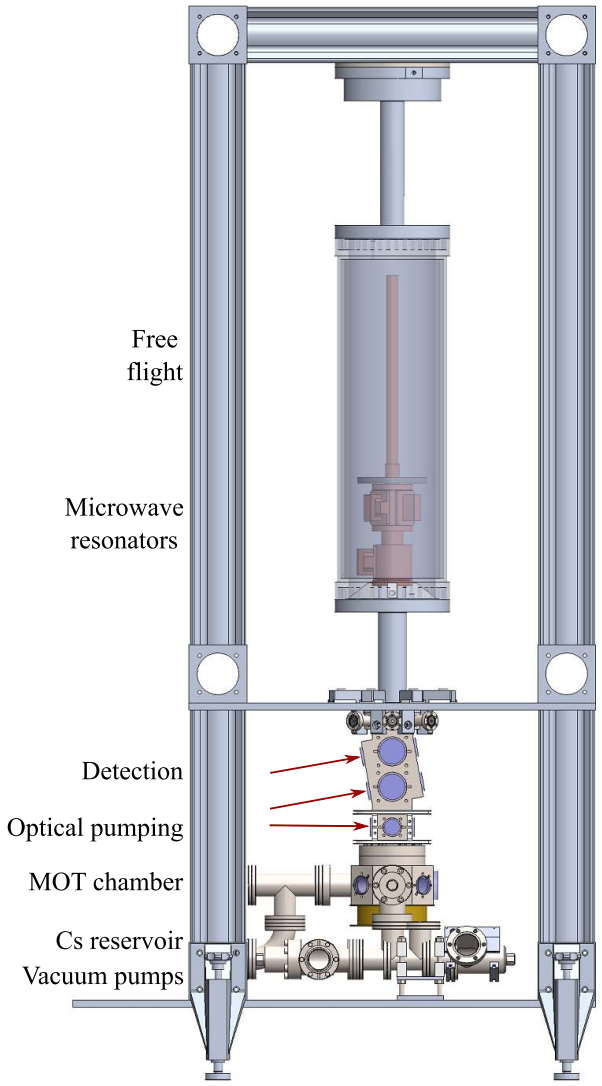

Fig. 3. Rendering of the physics package of the new fountains, excluding optics, microwave waveguides, C-field coil, upper MOT coil, and magnetic shields.

atoms then pass through the upper "Ramsey" cavity where a continuous microwave field induces the first $\pi/2$ pulse of a Ramsey sequence. The atom cloud reaches the apex of its flight under gravity about 30 cm above the Ramsey cavity, leading to a free precession time of 500 ms before the downward pass through the cavity and a second $\pi/2$ rotation of the state vector on the Bloch sphere about an axis that depends on the frequency of the microwaves relative to the atomic transition frequency. The two microwave interactions produce Ramsey fringes with a full width at half maximum of 1.0 Hz. The actual microwave field amplitude is intentionally varied by a small amount from the nominal $\pi/2$ value. This tuning of the microwave amplitude, together with the aforementioned tuning of the initial cloud size, is used to minimize the cold-collision frequency shift [21], [22]. The effective local collision energy between atoms during the Ramsey interaction is set such that collisions with atoms in the $F = 3$ state lead to frequency shifts with similar magnitude but opposite sign to those with atoms in the $F = 4$ state. This approach allows us to improve dramatically the usual tradeoff between short-term stability, which improves as the number of atoms probed is increased, and accuracy, which can be degraded by density-dependent frequency shifts. The small variation, typically a few percentage, of the microwave amplitude from the $\pi/2$ value introduces a slight reduction in fringe contrast, but the effect on the short-term stability is negligible.

The transition probability is measured after the atoms have left the microwave interrogation region by detecting the final atomic state populations. The fraction of signal from atoms in the $F = 4$ state relative to the total detected signal from all atoms gives a normalized transition probability that is insensitive to variations in the number of atoms. The microwave frequency is tuned symmetrically to either side of the central Ramsey fringe at the nominal atomic resonance, and any deviation of the local oscillator frequency is extracted from the difference in measured transition probabilities. This measured deviation is then fed back to the local oscillator as a correction for the following measurement cycle. The corrections are stored for postprocessed statistical analysis. Note that in this "fringe tracking" mode, the fountain does not provide a physical realization of standard frequency but monitors the local oscillator. This allows for convenient checks of leveraged systematic effects—for example, interleaved measurements at high and low density are used to measure and compensate for residual collisional shifts, which are typically 10^{-15} or less.

III. System Design

A. Physics Package Refinements

The new physics package design combines various features from the currently operational NPL fountains and includes a number of upgrades designed to improve the signal-to-noise ratio (SNR), reliability, resilience to systematic shifts, and transportability.

1) Signal-to-Noise Ratio Optimization: The SNR of the new fountains operating at low atom density has been improved by a modified Cs pumping system. The Cs vapor pressure in the trapping region is necessarily high to allow rapid loading of the MOT, but the presence of thermal Cs atoms in the neighboring detection region leads to an unwanted background fluorescence rate. Fluctuations in this fluorescence rate add noise to the measurement of the cold atom states and, hence, degrade the measurement SNR, especially when working with low atom numbers. Collisions with these hot Cs atoms also scatter cold atoms from the launched cloud, reducing the measured signal. The inclusion of shaped graphite getters between the MOT, detection, and microwave interaction regions suppresses both of these effects [23]. In each case, a central bore allows the launched cold atoms to pass through, while the large graphite surface area provides passive pumping of thermal cesium atoms. The shape of the graphite getter between the MOT and detection sections is optimized to improve on the background gas pumping provided by the active ion and getter pumps.

A secondary benefit of this graphite getter is that it partially collimates the thermal Cs atoms that are able to pass through it into a low-divergence beam. The detection axis of the new

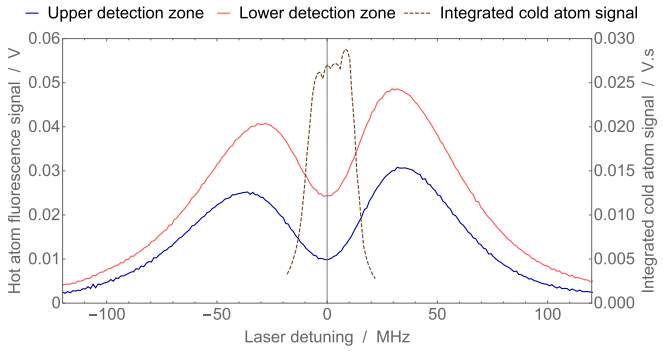

Fig. 4. Reduction in thermal background Cs fluorescence signal near resonance in both the top and bottom detection regions as a result of the 10° tilt of the detection probe beams for AOS-CsF1. The cold atoms' fluorescence is observed when the laser is tuned close to resonance, in between the Doppler shifted peaks of the thermal Cs fluorescence.

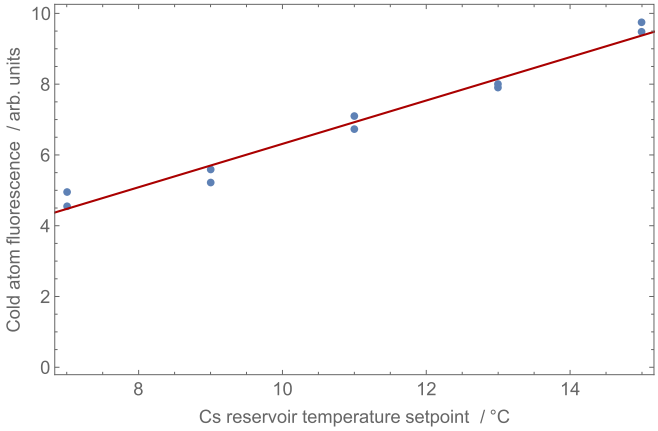

Fig. 5. Variation in observed cold-atom signal as a function of the Cs reservoir temperature setpoint of AOS-CsF1.

fountain design is tilted by 10° so that the probe lasers no longer propagate in the horizontal plane. This means that the absorption frequencies of the thermal Cs atoms are Doppler shifted away from those of the cold atoms—whose velocities are too small to exhibit significant Doppler shifts [24].

Spectra showing the frequency dependence of the fluorescence rate from hot background Cs atoms in each detection zone are presented in Fig. 4. The two peaks in each spectrum correspond to Doppler-broadened absorption from the forward and retro-reflected probe beams, and the splitting of the line centers is about 65 MHz. Also, shown in Fig. 4, is the spectrum of fluorescence from the cold Cs atoms as they fall through the detection region. These data were recorded separately by stepping the laser frequency between successive cycles of the fountain. The peak for the cold atoms is narrow, approximately 20 MHz, and is centered on the dip between the two background fluorescence peaks.

The new fountain design features seven separate pairs of coils in the MOT and optical pumping regions that allow us to precisely tailor the magnetic field during each stage of the fountain cycle. In addition to the MOT coils, there are three pairs of coils to cancel external fields, a pair of coils to generate a pulsed vertical field during optical pumping, and two pairs of coils that generate a small constant vertical magnetic field to provide a well-defined quantization axis as the atoms transition into the magnetically shielded section. This high degree of control of the magnetic fields experienced by the atoms ensures efficient optical pumping and transfer of the spin-polarized atomic sample into the flight tube and, hence, increases the number of atoms probed in the fountain.

2) Improved Reliability and Long-Term Operation: All of the required laser beams are delivered to the fountain by optical fibers, and the prealigned beam shaping and polarization optics are rigidly mounted onto the vacuum chamber. Besides being extremely stable, this arrangement enables us to transport the fountain without disassembly of the optical systems. The power of each of the nine laser beams is monitored with a photodiode and is continually logged by a monitoring system, which also records the feedback signals that stabilize the laser frequencies. This system makes it possible to identify any reduction in performance before it has a significant impact on the operation of the fountain. The power of each of the two probe beams is actively stabilized by varying the power of the radio frequency drives of acousto-optic modulators (AOMs) in their beam paths.

Maintaining a constant Cs vapor pressure in the MOT region helps stabilize the number of atoms that are trapped and probed in the fountain, and hence suppresses the small fluctuations in frequency shifts due to cold atom collisions and variations in signal levels. Excessive vapor pressure can also limit the lifetime of the ion pumps and the cesium source. In the new fountain design, the temperature of the Cs reservoir is actively stabilized by a regulator feeding back to a thermoelectric cooler mounted to the side of the reservoir. This system limits long-term fluctuations in temperature to about 0.1 K.

The reservoir temperature can also be used to controllably vary the vapor pressure of cesium in the MOT loading region, and hence the number of atoms launched in each fountain cycle. Fig. 5 shows the detected atom signal as the reservoir temperature is stepped up from 7 °C to 15 °C and back. The time constant for the vapor pressure to settle is about an hour, so for these measurements, the reservoir was left for several hours at each temperature. Over this measurement range, the change in the number of detected atoms varies approximately linearly with temperature. In the fountain used to record these data, the operating temperature is 8 °C. The fit indicates that at this point regulation to within 0.1 K corresponds to control of temperature-related atom number fluctuations at the level of about 1.2% in the long term, and significantly better on short timescales.

The other significant cause of atom number fluctuation is variation in the power and polarization of the laser beams delivered to the fountain. The new optical systems, described as follows, are designed to minimize these variations. The combination of reservoir temperature control and optical stability leads to the excellent atom number stability shown for NPL-CsF3 and AOS-CsF2 in Fig. 6.

3) Improved Systematic Shift Control: The physics package includes three nested layers of cylindrical mu-metal magnetic shielding to shield the atoms from external magnetic

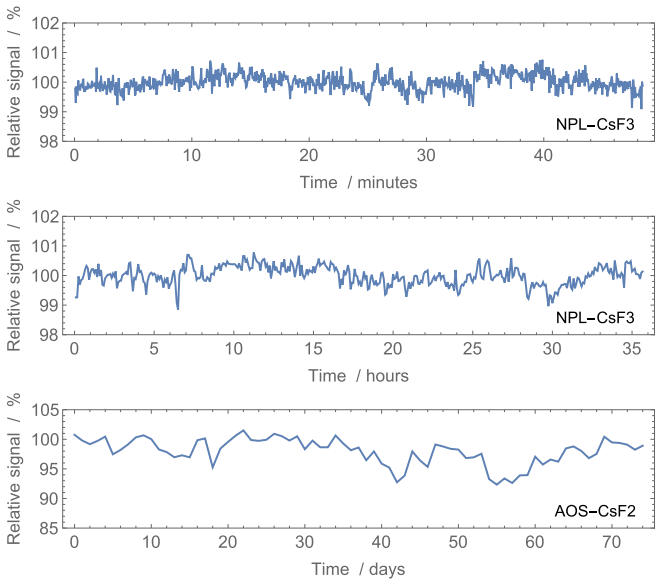

Fig. 6. *Top plots:* Relative cold atom fluorescence signal measured continuously in NPL-CsF3. The signal over the whole period is stable at the 1% level, compatible with the expected temperature stability of the Cs reservoir. *Bottom plot:* Signal recorded in AOS-CsF2 over 75 days without optimization, showing slightly larger fluctuations consistent with slow variations in laser power.

fields during the microwave interrogation. The applied C-field is designed to be homogeneous and stable and vertically aligned. External magnetic fields will change the magnitude of the magnetic field and shift the atomic frequency via the second-order Zeeman shift and can also tilt the angle of the C-field vector. The two relevant parameters for the shielding are, therefore, the residual field within the shields when no C-field is applied and the attenuation factor of external fields, both of which can be determined from the Zeeman splitting of the magnetic sublevels observed in Rabi microwave spectra of the atoms using single microwave pulses as they pass through one of the cavities. We have measured these as successive layers of shielding are applied, at each stage degaussing the shields to remove any magnetism induced in the shields themselves.

The residual field with one layer of shielding was found to be 14 nT at the Ramsey cavity but 120 nT at the selection cavity, suggesting that there is a significant gradient close to the apertures at the bottom and top of the shields. With two layers of shielding, the residual field at the Ramsey cavity is measured to be about 2 nT, with an even smaller difference between the two cavities. This is negligible compared to the 100-nT C-field that we would typically apply and is already sufficient for fountain operation.

The attenuation factor with a single set of shields is estimated to be about 2000 at the Ramsey cavity. With two sets, this increases to approximately 20 000—sufficiently large that the second-order Zeeman shift would be stable enough for accurate fountain operation in most laboratory environments. With all three shields installed, measurements have indicated an attenuation factor in the region of 50 000–100 000. This enables these fountains to operate even in noisy magnetic environments.

The Ramsey microwave resonator assembly, described in [17], is carefully designed to minimize the distributed cavity phase (DCP) effects that can cause frequency shifts for atoms whose trajectories are not perfectly vertical [25], [26]. The cavity resonates on the TE_{011} mode and microwaves can be injected from any of four waveguides oriented at right angles to each other. By feeding symmetrically from an opposing pair of waveguides, the lowest order DCP shifts, related to an $m = 1$ dipolar phase distribution, can be suppressed. Alternatively, by injecting microwaves from one feed at a time, it is possible to use the measured DCP frequency shifts as a diagnostic tool to determine the verticality of the atomic trajectories [16]. Effects related to the $m = 2$ quadrupolar phase distribution are minimized by orienting the feeding waveguides at 45° to the atom detection axis [26], [27].

The arrangement of the waveguide assembly is carefully designed to minimize microwave leakage. As a further measure to eliminate frequency shifts due to stray microwaves, a microwave cutoff tube fixed to the top of the Ramsey cavity extends up beyond the apex of the atomic trajectories. Any residual field propagating along this tube is rapidly attenuated to negligible levels. Similarly, a second cutoff tube reduces the coupling of microwaves between the Ramsey and selection cavities. The attenuation by this tube is approximately −50 dB and using the atoms as a probe of the microwave field, we have confirmed that the overall coupling between the two cavities is smaller than this. The atoms can still be exposed to a leakage field in the section between the selection cavity and detection chamber, but during this phase of their flight, the microwave frequency can be rapidly detuned far from the resonance. The entire cavity assembly is rigidly fastened to the frame on isolating mounts to prevent dc currents from generating uncontrolled magnetic fields.

To maintain ultra-high vacuum throughout the vacuum system, active getter pumps and ion pumps are installed at both the bottom and top of the system. After bake-out and activation of the pumps, the residual background pressure settles in the low 10^{-11} mbar range. While chemically active gases are efficiently removed by the getter pumps, the ion pumps are necessary to remove noble gases. With the ion pumps turned off, we observe a decay in the cold-atom signal with a time constant of over an hour. This slow decay is useful for evaluating frequency shifts due to collisions with background gas [28], [29].

4) Transportability: At 90 × 60 × 205 cm, the physics package is shorter and has a smaller footprint than previous Cs fountains built at NPL. To improve transportability, it also has increased rigidity and mechanical stability. Combined with the rigidly attached optics, this allows the fountains to be deployed immediately after transport, though full operation requires assembly and degaussing of the magnetic shields and an approximate vertical alignment. The two complete fountain systems AOS-CsF1 and AOS-CsF2 were delivered by road to AOS in Borowiec, Poland, and PSNC in Poznań, Poland. The ion pumps on these systems were operating during transport. Cold-atom signal was observed in each of these fountains on the same day it was delivered and initial microwave frequency measurements were performed within 2 days.

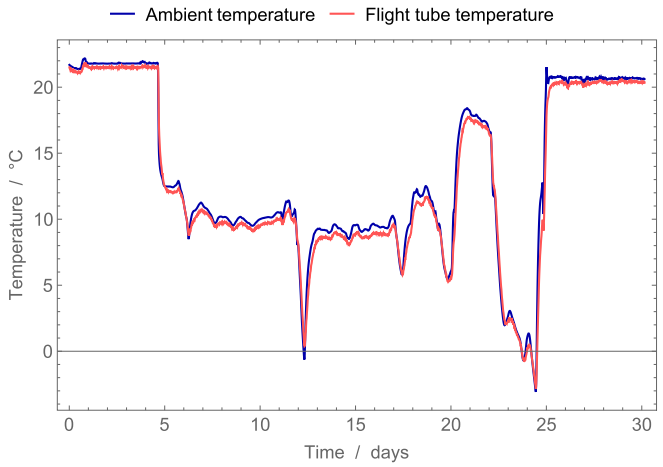

Fig. 7. Ambient and flight tube temperatures measured during transport by road and air from Teddington to Ottawa.

The NRC-FCs2 physics package was transported by air to NRC in Ottawa, ON, Canada. The new fountains contain a sufficient quantity of cesium that current aviation regulations require it to be removed before transport. The arrangement of valves on the physics package allows the cesium to be replaced without venting the complete system. Regulations also forbid the transport of cargo containing high voltages, preventing the use of ion pumps. The system sent to NRC was, therefore, pumped only by the passive getter pumps for approximately 4 weeks, after which the ion pumps were started without problems. Air transport also exposes the fountain to rapid changes in temperature. Fig. 7 shows the ambient and flight tube temperatures recorded during transport from NPL in Teddington, U.K. to NRC in Ottawa, ON, Canada. The combination of vibrations, rapid temperature changes, and only passive pumping has not led to any observed degradation in vacuum or fountain performance.

B. Optical and Electronic Systems

As with other transportable clock systems [24], the optical system that generates the various laser beams required for cooling, trapping, launching, optical pumping, and probing the atoms in the fountain has been designed to be compact and to provide excellent long-term frequency and amplitude stability. It consists of a 45×60 cm laser and spectroscopy unit connected by optical fibers to a 60×60 cm light distribution module. Instances of this system are currently being used with AOS-CsF1, AOS-CsF2, NPL-CsF2, and NPL-CsF3.

The primary laser is an extended cavity diode laser amplified by a tapered amplifier, with a distributed feedback laser used for the repumper. A small amount of the light from each laser is used for cesium vapor cell saturated absorption spectroscopy. Both lasers are frequency modulated at 1 MHz via their drive current, and the saturated absorption signals are demodulated to generate high-SNR error signals used to lock the laser frequencies to the appropriate transitions. In the case of the primary laser, an AOM before the spectroscopy setup is used to add a computer-controlled frequency shift that effectively changes the locking point of the laser. This offset locking system allows us to carry out rapid frequency tuning of the system without affecting the output power of the system. The locking systems remain continuously locked for months at a time without maintenance.

The majority of the light from each laser is coupled into optical fibers for transmission to the light distribution module. This contains all of the beamsplitters and polarization control necessary to produce the nine different beams that are sent via optical fiber to the fountain. Six AOMs are used to control the frequency and power of the various beams as required for the different stages of the fountain cycle. Spring-free, solenoid-based mechanical shutters, on padded mounts to minimize vibrations, extinguish the cooling light during the microwave interrogation. To improve the SNR of the detection process, AOMs in the probe beam paths actively stabilize the power in the fluorescence detection region. The MOT beams are not actively stabilized, but the optical system is designed such that small changes in alignment or input power tend to symmetrically affect the trapping and cooling beams to suppress the influence on atom number. These systems are extremely robust and have required no realignment after transport. Slight beam pointing drift in the commercial laser heads means that the coupling into the fibers leading to the distribution module needs optimization after several months. The reduction in coupling efficiency after this period is about 10%–15%. The light distribution modules themselves are extremely stable—the units operating at NPL have required no optimization since installation 15 months ago.

The new fountains are controlled by electronics that fit into a half-height 19 in rack. All the components for experimental control and data acquisition are combined into a single computer-controlled module. Dual laser frequency servos, a laser power monitor and stabilization unit, a reservoir temperature controller, and a simple state-selection microwave source have also been developed.

IV. System Performance

The quantum projection noise (QPN) of the detected atoms scales as $1/\sqrt{n_{\mathrm{det}}}$, where n_{det} is the number of atoms detected. The collisional shift cancelation enables us to use a relatively large number of atoms from a high-density MOT and, hence, obtain excellent SNR with a simple fountain design. We define the SNR as the inverse of the Allan deviation of the measured $F = 4$ fraction for successive cycles of the fountain, using resonant microwave that produces $2 \times \pi/4$ rotations such that the overall transition probability is approximately 0.5. The use of resonant microwaves suppresses the effect of frequency noise and, hence, removes the effect of the local oscillator from the measurement. Fig. 8 shows the measured SNR of the AOS-CsF1 fountain system plotted against the square root of the detected signal, which is proportional to $\sqrt{n_{\mathrm{det}}}$. Ideally, the data would follow the dashed line in Fig. 8. In addition to the QPN component, the model fit to the data includes a constant technical noise term, which on this square-root plot axis gives rise to a parabolic trend at low atom number, and a component proportional to the detected atom signal,

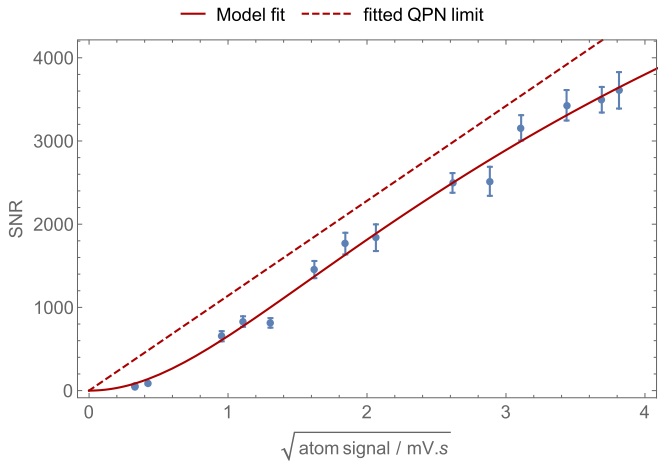

Fig. 8. Measurements of the signal-to-ratio as a function of the detected cold-atom fluorescence in AOS-CsF2 before shipment from NPL. Solid line: fit to the noise model described in the text. Dashed line: QPN limit extracted from the fit. Similar performance has been measured in all of the fountains that we have described here.

which leads to saturation of the SNR at high atom numbers. The fit indicates that the noise in detection is dominated by technical noise at low atom numbers, due primarily to shot noise in the amount of laser light scattered in the detection optical system. This can be substantially improved through the addition of apertures in the probe beams. The fit also suggests that saturation, due to noise sources such as frequency or amplitude noise on the detection lasers, is not significant except at the largest atom numbers.

For the highest atom numbers, we observe SNRs in excess of 3600, which are within 15% of the QPN limit. For the fountain duty cycle and Ramsey times used in these fountains, this corresponds to a short-term stability limit below $2.5 \times 10^{-14}/\sqrt{\tau}$. Measurements with an ultralow noise local oscillator in NPL-CsF3 showed a short-term stability of $3.5 \times 10^{-14}/\sqrt{\tau}$, consistent with its slightly poorer SNR of 2500. For measurements using most commercially available local oscillators, high-frequency microwave noise will limit the short-term stability to much higher values. Fig. 9 shows the measured Allan deviation curves for sequences of frequency measurements of a maser-referenced synthesizer[1] recorded using NRC-FCs2. The two different data sets correspond to operation of the fountain with an eightfold difference in the atom number. The short-term stabilities scale as $1.0 \times 10^{-13}/\sqrt{\tau}$ and $1.2 \times 10^{-13}/\sqrt{\tau}$, indicating that the fountain does not significantly limit the stability even at the lower atom number.

Accuracy evaluations of the three fountain systems that have been built are currently underway and will be described in detail elsewhere. We have, however, tested for agreement between NPL-CsF3 and the new systems for short periods while they were being optimized at NPL before transport. Fig. 10 shows the results of a comparison with AOS-CsF2 over an 8-day period. Both fountains were operated

[1]Vremya-CH-1003M, low-noise option.

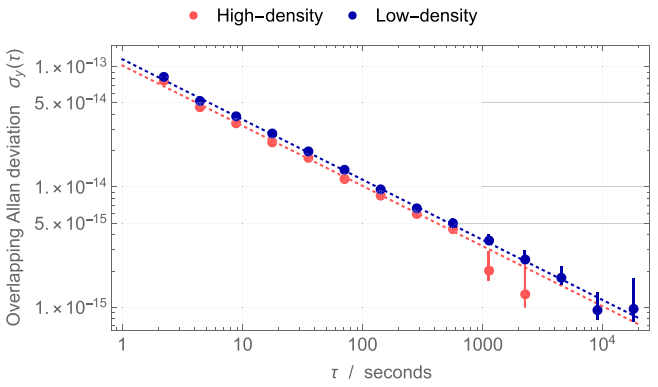

Fig. 9. Allan deviation plot of the short-term stability of NRC-FCs2 running at both high and low atom number. Red dashed line: $1.02 \times 10^{-13}/\sqrt{\tau}$. Blue dashed line: $1.17 \times 10^{-13}/\sqrt{\tau}$.

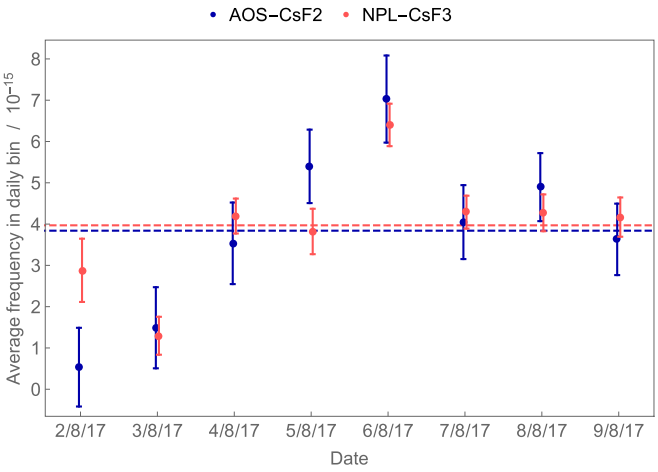

Fig. 10. Daily frequency measurements of the same maser by NPL-CsF3 and AOS-CsF2 over an 8-day period, showing overall agreement within the statistical uncertainty of 4×10^{-16}.

with quartz-based local oscillators of the same type and agree within the combined overall statistical uncertainty of 4×10^{-16}.

Preliminary checks of the leading systematic effects, such as the second-order Zeeman, blackbody radiation, and ac Stark shifts, indicate that type-B uncertainties comparable to the established NPL systems are achievable.

The NPL fountains have both been upgraded to use the new optical and electronic control systems, which have improved their uptime to almost 98%. The remaining downtime is most frequently caused by laser beam pointing instability reducing the amplitude of the laser frequency lock error signals. This problem could be overcome through fiber delivery of the spectroscopy beams.

V. Conclusion

We have demonstrated the capabilities of an improved cesium atomic fountain design building on the previous NPL fountains that use a simple vapor loaded MOT and collisional shift cancelation. Through commercial and scientific collaboration, several such systems have now been built, shipped to, and commissioned at international timing labs. The systems

are transportable and demonstrated robust operation in normal laboratory conditions. Measurements of the fountain SNR show that they can reach short-term stabilities in the low 10^{-14} range at 1 s, and they are expected to achieve accuracies similar to the established NPL systems.

ACKNOWLEDGMENT

The authors would like to thank S. Lea, W. Chen, J. Kronjäger, and D. Gentle for their valuable assistance during various stages of this work.

REFERENCES

[1] The United Kingdom Government Office Science. (2018). *Satellite-Derived Time and Position: A Study of Critical Dependencies*. [Online]. Available: https://www.gov.uk/government/publications/satellite-derived-time-and-position-blackett-review

[2] K. Turza, P. Krehlik, and Ł. Śliwczyński, "Long haul time and frequency distribution in different DWDM systems," *IEEE Trans. Ultrason., Ferroelectr., Freq. Control*, vol. 65, no. 7, pp. 1287–1293, Jul. 2018.

[3] E. F. Dierikx *et al.*, "White rabbit precision time protocol on long-distance fiber links," *IEEE Trans. Ultrason., Ferroelectr., Freq. Control*, vol. 63, no. 7, pp. 945–952, Jul. 2016.

[4] G. Offermans *et al.*, "eLoran initial operational capability in the United Kingdom—First results," in *Proc. Int. Tech. Meeting Inst. Navigat.*, Jan. 2015, pp. 27–39.

[5] A. Dammann, R. Raulefs, and S. Zhang, "On prospects of positioning in 5G," in *Proc. IEEE Int. Conf. Commun. Workshops (ICCW)*, Jun. 2015, pp. 1207–1213.

[6] S. Peil, T. B. Swanson, J. Hanssen, and J. Taylor, "Microwave-clock timescale with instability on order of 10^{-17}," *Metrologia*, vol. 54, no. 3, pp. 247–252, 2017. [Online]. Available: http://stacks.iop.org/0026-1394/54/i=3/a=247

[7] A. Bauch, S. Weyers, D. Piester, E. Staliuniene, and W. Yang, "Generation of UTC(PTB) as a fountain-clock based time scale," *Metrologia*, vol. 49, no. 3, pp. 180–188, 2012. [Online]. Available: http://stacks.iop.org/0026-1394/49/i=3/a=180

[8] G. D. Rovera *et al.*, "UTC(OP) based on lne-syrte atomic fountain primary frequency standards," *Metrologia*, vol. 53, no. 3, pp. S81–S88, 2016. [Online]. Available: http://stacks.iop.org/0026-1394/53/i=3/a=S81

[9] R. Wynands and S. Weyers, "Atomic fountain clocks," *Metrologia*, vol. 42, no. 3, pp. S64–S79, 2005. [Online]. Available: http://stacks.iop.org/0026-1394/42/i=3/a=S08

[10] J. Guéna *et al.*, "Progress in atomic fountains at LNE-SYRTE," *IEEE Trans. Ultrason., Ferroelectr., Freq. Control*, vol. 59, no. 3, pp. 391–409, Mar. 2012.

[11] F. P. Dos Santos, H. Marion, S. Bize, Y. Sortais, A. Clairon, and C. Salomon, "Controlling the cold collision shift in high precision atomic interferometry," *Phys. Rev. Lett.*, vol. 89, no. 23, p. 233004, Nov. 2002. [Online]. Available: https://link.aps.org/doi/10.1103/PhysRevLett.89.233004

[12] K. Szymaniec and S. E. Park, "Primary frequency standard NPL-CsF2: Optimized operation near the collisional shift cancellation point," *IEEE Trans. Instrum. Meas.*, vol. 60, no. 7, pp. 2475–2481, Jul. 2011.

[13] T. P. Heavner *et al.*, "First accuracy evaluation of NIST-F2," *Metrologia*, vol. 51, no. 3, p. 174, 2014. [Online]. Available: http://stacks.iop.org/0026-1394/51/i=3/a=174

[14] M. Kazda and V. Gerginov, "Suppression of microwave leakage shifts in fountain clocks by frequency detuning," *IEEE Trans. Instrum. Meas.*, vol. 65, no. 10, pp. 2389–2393, Oct. 2016.

[15] G. Santarelli *et al.*, "Switching atomic fountain clock microwave interrogation signal and high-resolution phase measurements," *IEEE Trans. Ultrason., Ferroelectr., Freq. Control*, vol. 56, no. 7, pp. 1319–1326, Jul. 2009.

[16] J. Guéna, R. Li, K. Gibble, S. Bize, and A. Clairon, "Evaluation of Doppler shifts to improve the accuracy of primary atomic fountain clocks," *Phys. Rev. Lett.*, vol. 106, no. 13, p. 130801, Apr. 2011. [Online]. Available: https://link.aps.org/doi/10.1103/PhysRevLett.106.130801

[17] K. Gibble, S. N. Lea, and K. Szymaniec, "A microwave cavity designed to minimize distributed cavity phase errors in a primary cesium frequency standard," in *Proc. Conf. Precis. Electromagn. Meas. (CPEM)*, Jul. 2012, pp. 700–701.

[18] K. Szymaniec, S. E. Park, G. Marra, and W. Chałupczak, "First accuracy evaluation of the NPL-CsF2 primary frequency standard," *Metrologia*, vol. 47, no. 4, pp. 363–376, 2010. [Online]. Available: http://stacks.iop.org/0026-1394/47/i=4/a=003

[19] K. Szymaniec, S. N. Lea, K. Gibble, S. E. Park, K. Liu, and P. Głowacki, "NPL Cs fountain frequency standards and the quest for the ultimate accuracy," *J. Phys., Conf. Ser.*, vol. 723, no. 1, p. 012003, 2016. [Online]. Available: http://stacks.iop.org/1742-6596/723/i=1/a=012003

[20] K. Szymaniec, H.-R. Noh, S. E. Park, and A. Takamizawa, "Spin polarization in a freely evolving sample of cold atoms," *Appl. Phys. B, Lasers Opt.*, vol. 111, no. 3, pp. 527–535, May 2013, doi: 10.1007/s00340-013-5368-7.

[21] K. Szymaniec, W. Chałupczak, E. Tiesinga, C. J. Williams, S. Weyers, and R. Wynands, "Cancellation of the collisional frequency shift in caesium fountain clocks," *Phys. Rev. Lett.*, vol. 98, no. 15, p. 153002, Apr. 2007. [Online]. Available: https://link.aps.org/doi/10.1103/PhysRevLett.98.153002

[22] K. Szymaniec, W. Chałupczak, S. Weyers, and R. Wynands, "Prospects of operating a caesium fountain clock at zero collisional frequency shift," *Appl. Phys. B, Lasers Opt.*, vol. 89, nos. 2–3, pp. 187–193, Nov. 2007, doi: 10.1007/s00340-007-2813-5.

[23] A. Clairon, P. Laurent, G. Santarelli, S. Ghezali, S. N. Lea, and M. Bahoura, "A cesium fountain frequency standard: Preliminary results," *IEEE Trans. Instrum. Meas.*, vol. 44, no. 2, pp. 128–131, Apr. 1995.

[24] P. Laurent *et al.*, "Design of the cold atom PHARAO space clock and initial test results," *Appl. Phys. B, Lasers Opt.*, vol. 84, no. 4, pp. 683–690, Sep. 2006, doi: 10.1007/s00340-006-2396-6.

[25] R. Li and K. Gibble, "Phase variations in microwave cavities for atomic clocks," *Metrologia*, vol. 41, no. 6, p. 376, 2004. [Online]. Available: http://stacks.iop.org/0026-1394/41/i=6/a=004

[26] R. Li and K. Gibble, "Evaluating and minimizing distributed cavity phase errors in atomic clocks," *Metrologia*, vol. 47, no. 5, p. 534, 2010. [Online]. Available: http://stacks.iop.org/0026-1394/47/i=5/a=004

[27] R. Li, K. Gibble, and K. Szymaniec, "Improved accuracy of the NPL-CsF2 primary frequency standard: Evaluation of distributed cavity phase and microwave lensing frequency shifts," *Metrologia*, vol. 48, no. 5, p. 283, 2011. [Online]. Available: http://stacks.iop.org/0026-1394/48/i=5/a=007

[28] K. Gibble, "Scattering of cold-atom coherences by hot atoms: Frequency shifts from background-gas collisions," *Phys. Rev. Lett.*, vol. 110, no. 18, p. 180802, May 2013. [Online]. Available: https://link.aps.org/doi/10.1103/PhysRevLett.110.180802

[29] K. Szymaniec, S. N. Lea, and K. Liu, "An evaluation of the frequency shift caused by collisions with background gas in the primary frequency standard NPL-CsF2," *IEEE Trans. Ultrason., Ferroelectr., Freq. Control*, vol. 61, no. 1, pp. 203–206, Jan. 2014.

Richard J. Hendricks (M'18), photograph and biography not available at the time of publication.

Filip Ozimek, photograph and biography not available at the time of publication.

Krzysztof Szymaniec, photograph and biography not available at the time of publication.

Bartłomiej Nagórny, photograph and biography not available at the time of publication.

Piotr Dunst, photograph and biography not available at the time of publication.

Jerzy Nawrocki, photograph and biography not available at the time of publication.

Scott Beattie, photograph and biography not available at the time of publication.

Bin Jian, photograph and biography not available at the time of publication.

Kurt Gibble, photograph and biography not available at the time of publication.